

Electronic Supplementary Information For

Upconversion Luminescence Enhancement of Yb³⁺,Nd³⁺ Sensitized NaYF₄ Core-Shell Nanocrystals on Ag Grating Film

Wen Xu,^a Hongwei Song,^{*a}Xu Chen,^aHaiyu Wang,^a Shaobo Cui,^{ab} Donglei Zhou,^a Pingwei Zhou,^a Sai Xu^a

^aState Key Laboratory on Integrated Optoelectronics, College of Electronic Science and Engineering, Jilin University, Changchun, 130012, People's Republic of China;

^bCollege of Physics, Jilin University, 2699 Qianjin Street, Changchun 130012, People's Republic of China.
Fax:86-431-85155129; Tel:86-431-85155129; E-mail: songhw@jlu.edu.cn.

Experimental section

The preparing process of the Ag gratings was as follows: firstly, the gratings were fabricated on NOA-63 polymer resist coated on glass substrates by the two-beam interference method. Then a 50 nm thick layer of silver was evaporated on top of the grating (evaporation rate 1 Å/s in a UHV chamber). As a comparison, the traditional Ag nano-film on the glass substrate was prepared by the same method. The NaYF₄:Yb³⁺,Tm³⁺@NaYF₄:Yb³⁺,Nd³⁺ core-shell NCs were prepared through the two-step thermal decomposition of rare earth chlorides in the Oleic acid (OA) and 1-octadecene (ODE). Then, the solvent evaporation method was used to assemble NaYF₄:Yb³⁺,Tm³⁺@NaYF₄:Yb³⁺,Nd³⁺ core-shell NCs layer-by-layer on the glass substrate and Ag gratings. As a comparison, NaYF₄:Yb³⁺,Nd³⁺@NaYF₄:Yb³⁺,Tm³⁺ core-shell NCs were also synthesized.

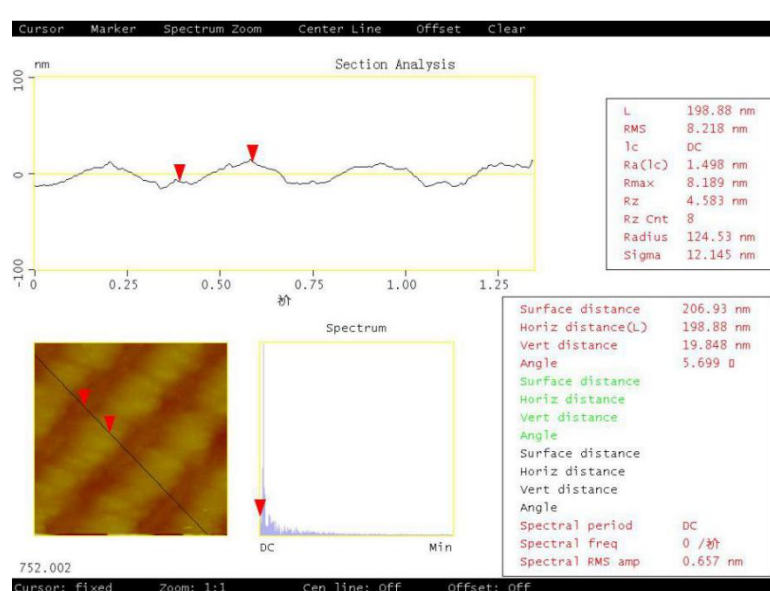


Fig.S1 The periods and depth analysis of Ag grating, respectively.

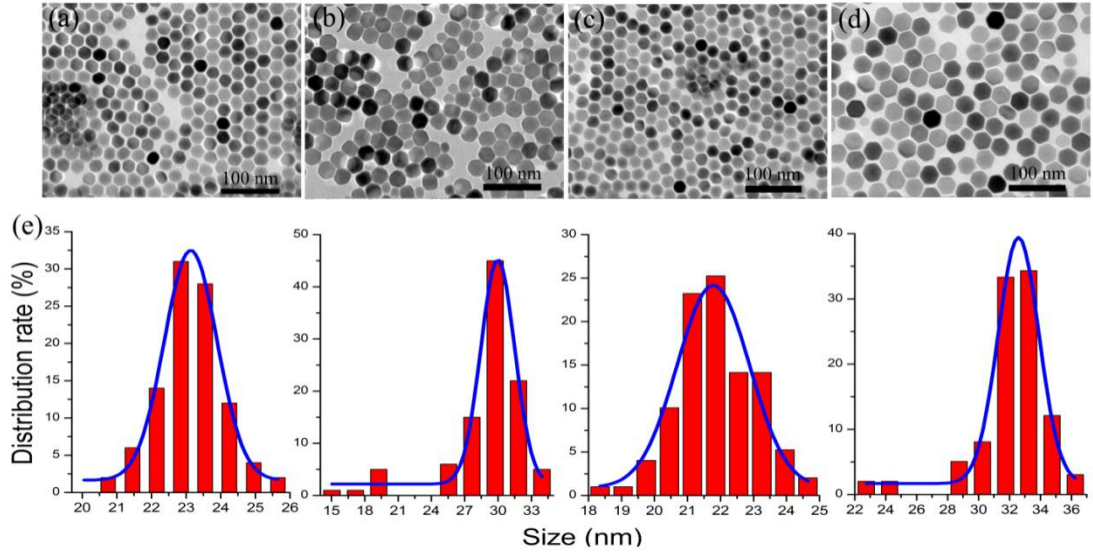


Fig.S2 (a-d) an (e) shows the TEM images of $\text{NaYF}_4:\text{Yb}^{3+},\text{Tm}^{3+}$, $\text{NaYF}_4:\text{Yb}^{3+},\text{Tm}^{3+} @ \text{NaYF}_4:\text{Yb}^{3+},\text{Nd}^{3+}$, $\text{NaYF}_4:\text{Yb}^{3+},\text{Nd}^{3+}$, $\text{NaYF}_4:\text{Yb}^{3+},\text{Nd}^{3+} @ \text{NaYF}_4:\text{Yb}^{3+},\text{Tm}^{3+}$ NCs, and the corresponding size distribution images, respectively.

In order to verify the forming of the core-shell structure, Fig.S2 (a-d) an (e) shows the TEM images of $\text{NaYF}_4:\text{Yb}^{3+},\text{Tm}^{3+}$, $\text{NaYF}_4:\text{Yb}^{3+},\text{Tm}^{3+} @ \text{NaYF}_4:\text{Yb}^{3+},\text{Nd}^{3+}$, $\text{NaYF}_4:\text{Yb}^{3+},\text{Nd}^{3+}$, $\text{NaYF}_4:\text{Yb}^{3+},\text{Nd}^{3+} @ \text{NaYF}_4:\text{Yb}^{3+},\text{Tm}^{3+}$ NCs, and the corresponding size distribution images, respectively. From Fig.S2, it's known that all the samples have highly uniform and monodispersed. And before homogeneous coating, the average size of $\text{NaYF}_4:\text{Yb}^{3+},\text{Tm}^{3+}$ and $\text{NaYF}_4:\text{Yb}^{3+},\text{Nd}^{3+}$ NCs as the core component are ~ 23 nm and ~ 22 nm, respectively. Then, the core-shell structure was further prepared by overgrowing a NaYF_4 shell layer on the core NCs. The average size of the as-obtained $\text{NaYF}_4:\text{Yb}^{3+},\text{Tm}^{3+} @ \text{NaYF}_4:\text{Yb}^{3+},\text{Nd}^{3+}$ and $\text{NaYF}_4:\text{Yb}^{3+},\text{Nd}^{3+} @ \text{NaYF}_4:\text{Yb}^{3+},\text{Tm}^{3+}$ NCs is 30 nm and 33 nm, implying the shell thickness with 3.5 nm and 5nm, respectively. We know that in the chemistry experiment, it is difficult to remain the as-prepared samples consistent at every time due to the influence of the experiment condition control, instrumental error and human factors, especially in nanoscale level. So the as-prepared samples have a subtle difference between the as-obtained $\text{NaYF}_4:\text{Yb}^{3+},\text{Tm}^{3+} @ \text{NaYF}_4:\text{Yb}^{3+},\text{Nd}^{3+}$ and $\text{NaYF}_4:\text{Yb}^{3+},\text{Nd}^{3+} @ \text{NaYF}_4:\text{Yb}^{3+},\text{Tm}^{3+}$ NCs.

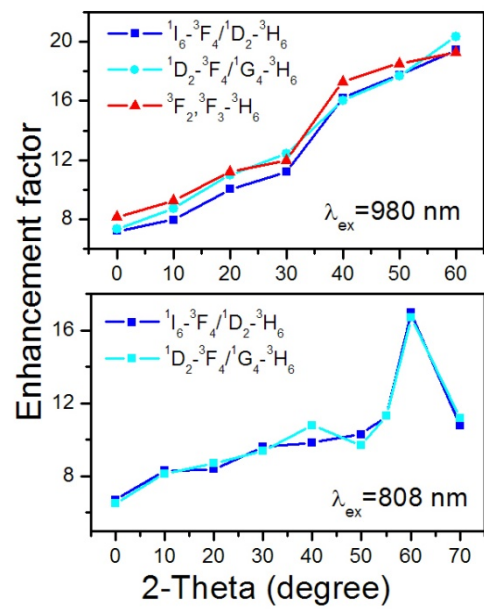


Fig.S3 The UCL EF of the different transitions as a function of the incident angle under 980 nm and 808 nm excitation, respectively.

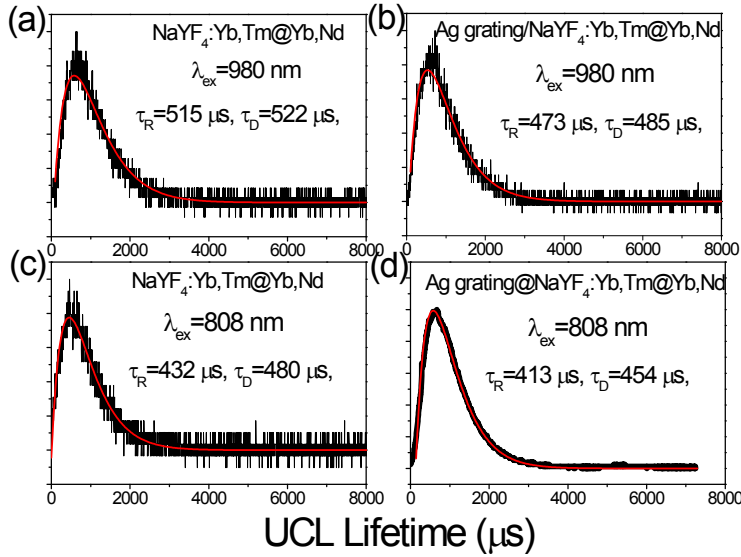


Fig.S4 The UCL dynamics of the ${}^1\text{G}_4$ - ${}^3\text{H}_6$ transition for NaYF₄:Yb,Tm @NaYF₄:Yb, Nd and Ag grating/NaYF₄:Yb,Tm @NaYF₄:Yb, Nd under 980 nm and 808 nm excitation, respectively.

Fig. S4 records the UCL process of the ${}^1\text{G}_4$ - ${}^3\text{H}_6$ transition for Tm³⁺ ions in different samples under 980 nm and 808 nm excitaiton, which can be well fitted be a double exponential function $I(t) = I_0 e^{-t/\tau_D} - I_0 e^{-t/\tau_R}$. It could be concluded that in the Ag grating/NaYF₄:Yb,Tm @NaYF₄:Yb, Nd composite film, in comparison to the pure NaYF₄:Yb,Tm @NaYF₄:Yb,Nd flim, the rising (τ_R) and decay (τ_D) time constants changed little under both 980 nm and 808 nm excitation, and the maximum variation was lower than 8%, suggesting that these transition rates nearly reserved as a constant.

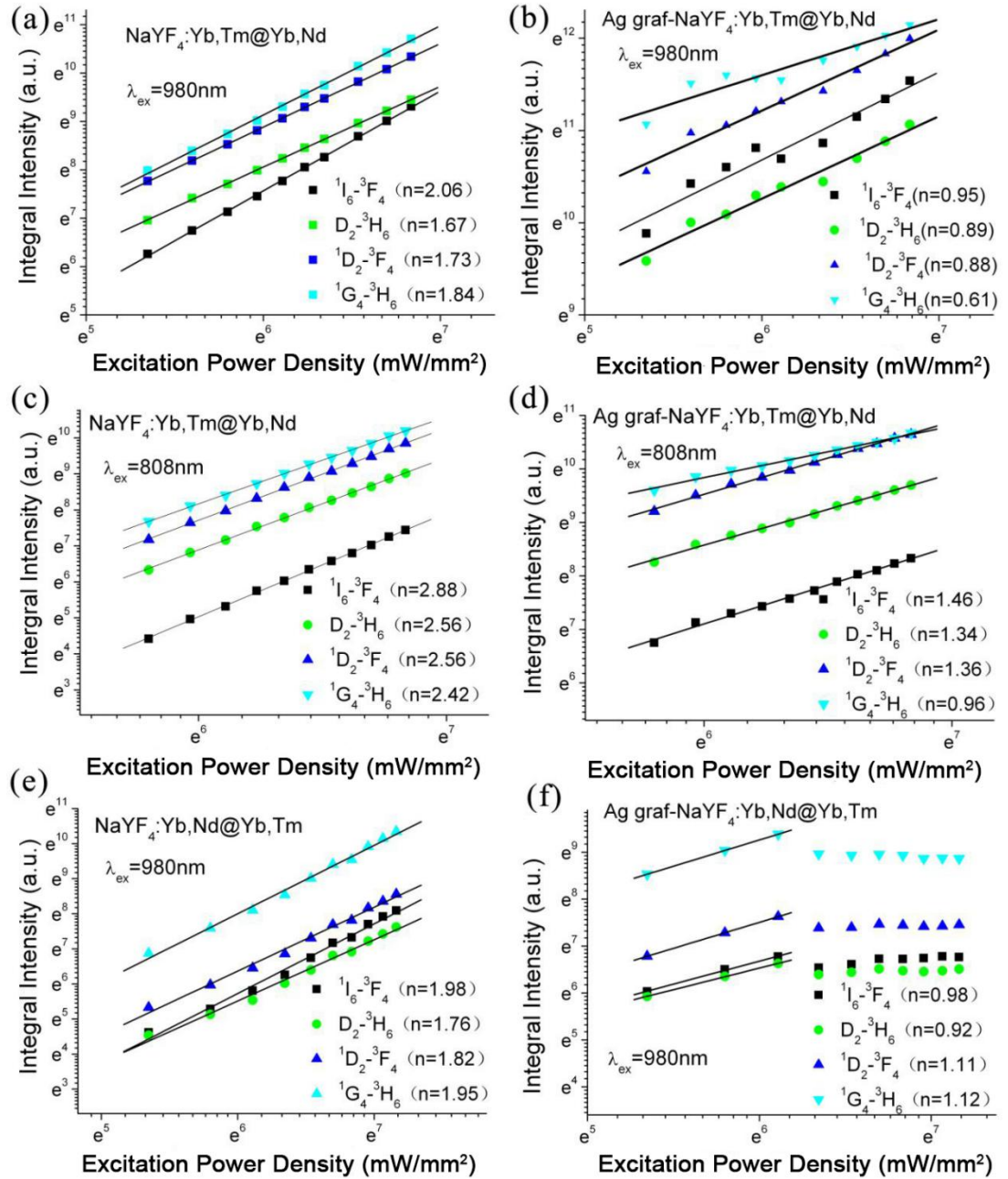


Fig.S5 The multicolor UCL intensity as a function of excitation power **density** in ln-Ln plot under 980 nm and 808 nm excitation: (a) $\text{NaYF}_4\text{-Yb}^{3+}\text{-Tm}^{3+}@\text{NaYF}_4\text{-Yb}^{3+}\text{-Nd}^{3+}$ under 980 nm excitation, (b) Ag grating / $\text{NaYF}_4\text{-Yb}^{3+}\text{-Tm}^{3+}@\text{NaYF}_4\text{-Yb}^{3+}\text{-Nd}^{3+}$ under 980 nm excitation, (c) $\text{NaYF}_4\text{-Yb}^{3+}\text{-Tm}^{3+}@\text{NaYF}_4\text{-Yb}^{3+}\text{-Nd}^{3+}$ under 808 nm excitation, (d) Ag grating/ $\text{NaYF}_4\text{-Yb}^{3+}\text{-Tm}^{3+}@\text{NaYF}_4\text{-Yb}^{3+}\text{-Nd}^{3+}$ under 808 nm excitation, (e) $\text{NaYF}_4\text{-Yb}^{3+}\text{-Nd}^{3+}@\text{NaYF}_4\text{-Yb}^{3+}\text{-Tm}^{3+}$ under 980 nm excitation, (b) Ag grating/ $\text{NaYF}_4\text{-Yb}^{3+}\text{-Nd}^{3+}@\text{NaYF}_4\text{-Yb}^{3+}\text{-Tm}^{3+}$ under 808 nm excitation, respectively.

In order to better understand the fact above, the multicolor UCL intensity as a function of excitation power **density** in ln-Ln plot was recorded, as shown in Fig. S3. Generally, UCL intensity as a function of excitation power **density** can be expressed as, $I_{\text{UCL}} \propto P_{\text{Laser}}^n$. It can be seen that the n values are all much smaller than the required photon numbers ($n = 2-5$) populating the $^1\text{G}_4$, $^1\text{D}_2$ and $^1\text{I}_6$ levels, which can be attributed to the saturation effect as well as thermal effect. It can be

seen that, in Fig S3(a-d), with the increase of the excitation power **density**, the UCL intensity gradually increases, and the n values for Ag grating/ $\text{NaYF}_4:\text{Yb}^{3+},\text{Tm}^{3+}$ @ $\text{NaYF}_4:\text{Yb}^{3+},\text{Nd}^{3+}$ composite film (Fig.3b and Fig.3d) is lower than that of the $\text{NaYF}_4:\text{Yb}^{3+},\text{Tm}^{3+}$ @ $\text{NaYF}_4:\text{Yb}^{3+},\text{Nd}^{3+}$ composite film (Fig.3a and Fig.3c) under **980 nm** and 808 nm excitation, respectively. Combing with the result in Fig 4, it would be attributed to the thermal effect of Ag grating, leading to the decrease of the EF. It should be noted that, in Ag grating/ $\text{NaYF}_4:\text{Yb}^{3+},\text{Nd}^{3+}$ @ $\text{NaYF}_4:\text{Yb}^{3+},\text{Tm}^{3+}$ composite film under 980 nm excitation (Fig.3f), as the excitation power **denisty** exceeds to **510mW/mm²**, the UCL intensity of Ag grating/ $\text{NaYF}_4:\text{Yb}^{3+},\text{Nd}^{3+}$ @ $\text{NaYF}_4:\text{Yb}^{3+},\text{Tm}^{3+}$ composite film obviously decreases as further increase the excitation power **density**. This phenomenon has not been observed in Ag grating/ $\text{NaYF}_4:\text{Yb}^{3+},\text{Tm}^{3+}$ @ $\text{NaYF}_4:\text{Yb}^{3+},\text{Nd}^{3+}$ composite film. In general, when Tm^{3+} locates in the shell, as the excitation power **density** exceeds **510mW/mm²**, the UCL intensity obviously quenches, due to the non-radiative significantly increase resulting of the thermal effect of laser radiation and photothermal converison of Ag grating, while it is not observed as Tm^{3+} locates in the core. It is natural, because the excitation power **density** locating in the core will decrease greatly due to the homogeneous doping of Yb^{3+} ions. Furthermore, as the luminescent centers locate in the core, because of the existence of the passivation shell, the thermal effect can be prevented to some **extend**.